

<https://doi.org/10.1038/s41612-025-01083-z>

Importance of fluvial inflows in the intra-lake heterogeneity of surface water temperatures on the Tibetan Plateau

Bingqing Du^{1,2}, Jing Zhou¹✉, Deliang Chen³, Hu Liu^{1,2}, Baoyan Liu^{1,2,4}, Ruishun Liu^{1,2} & Lei Wang^{1,2}✉

Lakes on the Tibetan Plateau (TP) are highly responsive to environmental change. Spatiotemporal variations in the lake surface water temperature (LSWT) significantly impact regional ecosystem stability, carbon cycling, and regional climate. However, due to limited observations, the intra-lake heterogeneity of LSWT and its driving forces remain unclear. By employing multi-source datasets, especially observation-constrained LSWT and lake inflow data, along with the random forest method, we analyzed three TP lakes (Nam Co, Siling Co, and Paiku Co) during 2001–2019. No evident inter-annual LSWT changes were detected. Lake inflow (up to 40% contribution) was the main driver of LSWT variations from July to November, followed by air temperature. Spatially, LSWT intra-lake heterogeneity varied among lakes, with Siling Co showing the largest difference (nearly 4 °C) in autumn, mainly caused by river inflow locations and lake bathymetry. This study improves our understanding of the spatiotemporal variations of LSWT for high-mountain lakes, providing insights for climate-change adaptation and water resources management.

Lakes contain 87% of global liquid freshwater¹ and act as regulators of the carbon cycle and climate². They play an important ecosystem services role and are sentinels of climate change³. The main focus of previous studies on the impacts of climate change on lakes include the loss of lake ice cover^{4–6}, accelerated lake evaporation⁷, and alteration of lake mixing regimes⁸. One of the most direct responses to current climate change is an increase in lake surface water temperature (LSWT)^{9–11}, which further impacts lake ecosystems¹² and greenhouse gas emissions¹³. Additionally, variations in LSWT influence atmospheric temperature and moisture at a local scale. Therefore, it is important to understand how lake temperatures vary in response to climate change.

The Tibetan Plateau (TP), often referred to as the “Asian Water Tower”, is experiencing rapid warming and is currently warmer than any time in the past 2000 years¹⁴. Under this changing climate, the area of lakes¹⁵ as well as water storage¹⁶ and water levels^{17–20} have changed during recent decades. These changes will inevitably affect fluctuations in lake temperatures. With the development of advanced measurement technologies, LSWT datasets^{21–23} have become available, facilitating the study of lake temperatures on the TP. Wan et al.²² calculated LSWT change rates for 374 lakes on the TP for the period 2001–2015, revealing contrasting patterns between nighttime and daytime: an overall trend of 0.37 ± 0.44 °C/decade at

night and -0.54 ± 0.51 °C/decade during the day. Using moderate resolution imaging spectroradiometer (MODIS) products, Zhang et al.²¹ analyzed temperature changes in 52 lakes on the TP over the period 2001–2012, revealing an overall increasing trend, with rates ranging from 0.01 to 0.47 °C/decade, although a few lakes (21 lakes) exhibited cooling trends.

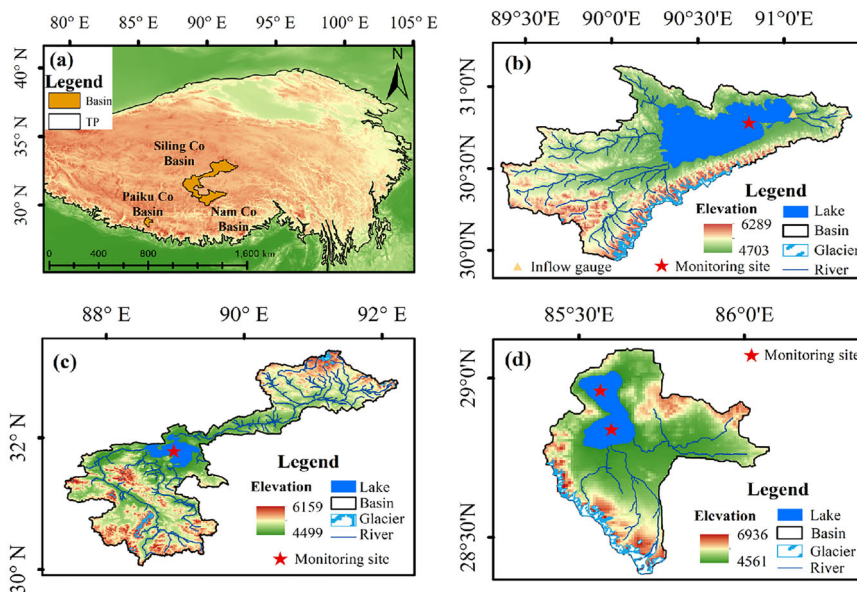
In general, LSWT is influenced by climatic factors, such as air temperature, solar radiation, cloud cover, and wind speed²⁴. Specifically, widespread increases in LSWT occur in response to atmospheric warming^{25–27}; increased solar radiation can increase LSWT during spring and summer²⁸; a decline in wind speed has been observed to increase LSWT by diminishing vertical mixing and surface turbulent heat fluxes within lakes^{8,29}; and increased specific humidity can raise LSWT by reducing the upward latent heat flux. In summary, air temperature, shortwave radiation, longwave radiation, and specific humidity have positive effects on LSWT, while wind speed has a negative effect on LSWT.

Many studies have explored the drivers of lake warming, aiming to understand the causes of lake temperature changes. Tong et al.⁷ quantified the contributions of key external climate-forcing parameters to global LSWT trends, finding that an increase in air temperature accounted for 47% of global lake warming, with other notable contributions from longwave radiation (26%) and specific humidity (25%). Huang et al.³⁰ found that

¹State Key Laboratory of Tibetan Plateau Earth System, Environment and Resources, Institute of Tibetan Plateau Research, Chinese Academy of Sciences, Beijing, China. ²University of Chinese Academy of Sciences, Beijing, China. ³Department of Earth System Science, Tsinghua University, Beijing, China. ⁴Resettlement Affairs Center for Large and Medium-sized Water Resources and Hydropower Projects of Tibet Autonomous Region, Lhasa, China.

✉ e-mail: zhoujing@itpcas.ac.cn; wanglei@itpcas.ac.cn

Fig. 1 | Overview of the study area. **a** Location of the study area on the Tibetan Plateau (TP). **b–d** Distribution of rivers and geography of the Nam Co, Siling Co, and Paiku Co basins, respectively. The red five-pointed stars indicate the locations of the in-situ monitoring sites of lake temperature. The yellow triangle indicates the in-situ flow monitoring point in Nam Co.



changes in air temperature, downward longwave radiation, and wind speed were the most important climatic drivers of LSWT changes in China. Most studies have emphasized the influence of climatic factors on temperature changes within lakes but have generally overlooked the key role of rivers flowing into lakes. For example, on the TP, the increasing rate of non-glacial-fed lakes is much higher than that of glacial-fed lakes, likely owing to cold water input from glacier melting³¹. Therefore, it is necessary to consider the role of river inflows into lakes when determining the causes of lake temperature changes, especially in high-elevation lakes.

Spatial distribution of LSWT provide important evidence in intra-lake increasing patterns. For example, in large lakes across the Northern Hemisphere, LSWTs in deep areas display higher rates of warming during summer, attributed to the greater temporal persistence in deep areas of temperature anomalies associated with an earlier onset of thermal stratification³². By analyzing the temperature differences in different regions, it is possible to clearly reveal the heat transfer pathways in the lake, the water mixing patterns, and the spatial differentiation of the living environment of aquatic organisms. This is crucial for constructing a comprehensive and accurate understanding of lake ecosystem, which is conducive to the rational utilization of lake resources and the important basis for the sustainable development of human society.

The major objective of this study is to identify and better understand the role of lake inflows in determining both the overall variations and intra-lake heterogeneity of LSWT from July to November. We selected three lakes (Nam Co, Siling Co, and Paiku Co) and their surrounding basins on the TP (Fig. 1), all having available in-situ lake temperature observations, as case studies. The random forest method was used to identify the main driving factors of LSWT changes in these three lakes. We also analyzed the relationships between the intra-lake heterogeneity of LSWT and both fluvial inflows and lake bathymetry.

Results

Evaluation of CCI-LSWT dataset

After comparison with in-situ observations at different points within the three lakes (Fig. 2), the CCI-LSWT dataset was shown to accurately reproduce the dynamics of LSWT. The minimum *r* between CCI-LSWT and observed LSWT exceeded 0.9, and the largest absolute values of mean bias and RMSE were 0.51 and 1.60 °C, respectively.

In addition, we validated the LSWT values from the CCI-LSWT dataset across entire lakes using MODIS data on a monthly scale. The comparison was conducted during the ice-free period when the CCI-LSWT dataset contains more available data. Accordingly, we selected May–December for

Nam Co³³, April–November for Siling Co³⁴, and April–December for Paiku Co³⁵. There was a strong correlation between CCI-LSWT and MODIS LSWT, with *r* exceeding 0.9 and absolute values of mean bias and RMSE not exceeding 1.66 and 2.15 °C, respectively (Fig. 3). However, an underestimation was observed in CCI-LSWT, which may be a result of the transit time of MODIS Terra generally being later in the day than that of the satellites producing the CCI-LSWT dataset, allowing more time for the lake to heat up. Overall, our evaluation demonstrates that the CCI-LSWT dataset can be applied to the analysis of LSWT in these three lakes.

Evaluation of lake inflow dataset

We collected available monthly average observed inflows of Nam Co Basin at Niyaqu River to evaluate the accuracy of the GRFR dataset for the period 2008–2012. Our results showed that the GRFR dataset can accurately capture the monthly variation in inflow discharge, with an *r* of 0.84 (Fig. 4). The relatively small mean bias of 0.43 m³/s and RMSE of 1.82 m³/s confirmed the accuracy of the GRFR dataset, this being sufficient for our focus on discharge changes here.

Contributions of hydroclimatic variables to LSWT

We calculated the mean LSWT of the whole lake from July to November for the period 2001–2019, as shown in Fig. 5. Using linear fitting, we found that the temperature variation in each of the three lakes was below 0.1 °C/decade and did not pass the 0.05 significance test. Despite the general increase in air temperature across the TP, the three lakes did not show a significant warming trend, so the influence of other hydrometeorological factors was investigated.

We explored the importance of 2-m air temperature, shortwave radiation, longwave radiation, wind speed, specific humidity, and river discharge to the changes in LSWT. Zero - phase component analysis was employed. Random forest analysis was used to quantitatively analyze the relative contributions of different variables in explaining the overall LSWT variations in the three lakes from July to November (Fig. 6). This analysis showed that > 85% of the variation in LSWT values can be attributed to meteorological variables and lake inflows. Specifically, river discharge was the most important factor explaining the changes in LSWT values (*p* < 0.01) in all lakes, with its RCR reaching 40%, exceeding the influence of meteorological factors. The water inputs to lakes from precipitation and glacier or snow meltwater typically have a lower temperature than the lake water, which can modulate lake temperature³¹. This may cause the three lakes do not exhibit significant interannual variation. In addition, air temperature and specific humidity also had a significant impact on overall lake temperatures (*p* < 0.05).

Fig. 2 | Comparison of daily lake surface water temperature (LSWT) (°C) between the CCI-LSWT dataset and observations in the three studied lakes. a Nam Co. **b** Siling Co. **c** Northern part of Paiku Co. **d** Southern part of Paiku Co. RMSE root-mean-square error, *r* correlation coefficient, *n* data volume.

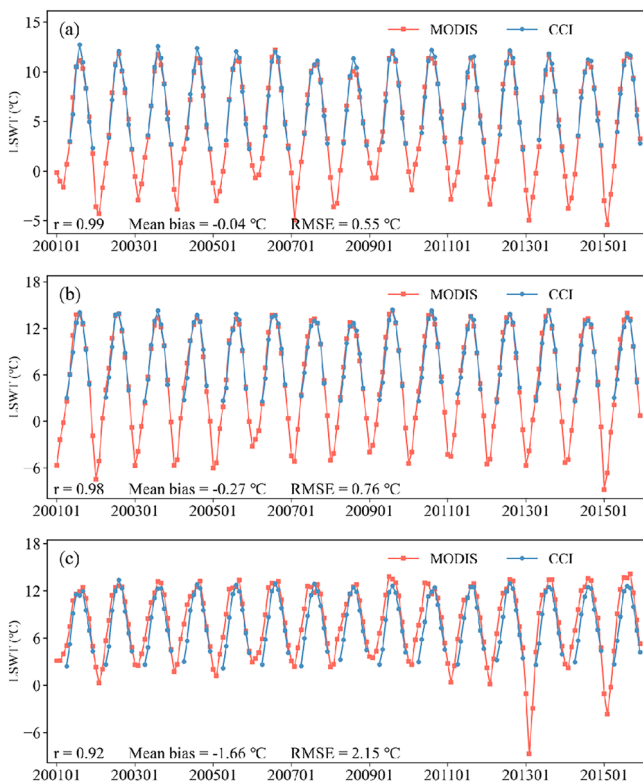
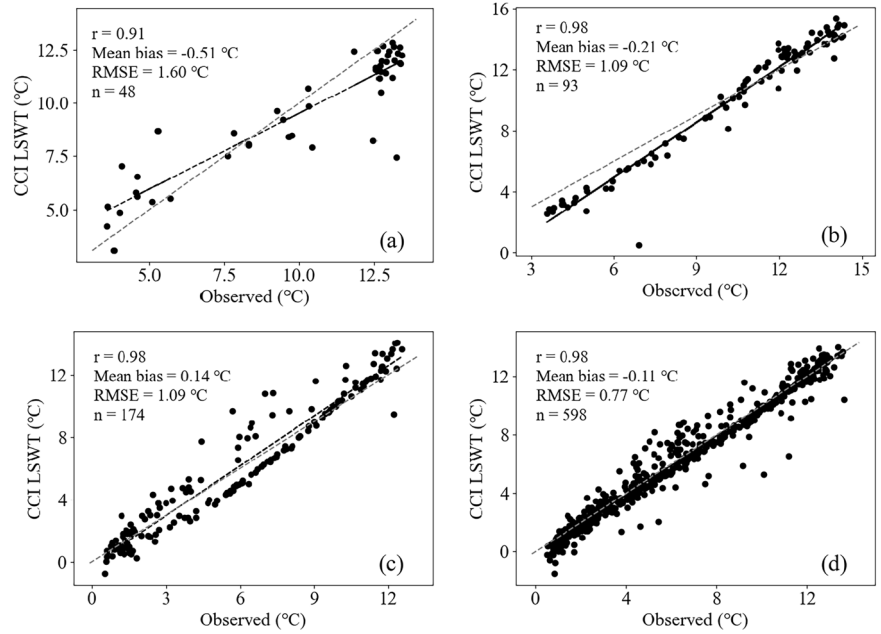


Fig. 3 | Interannual variation of monthly lake surface water temperature (LSWT) of CCI (blue line) and moderate resolution imaging spectroradiometer (MODIS) data (red line) during the period 2001–2019. a Nam Co. **b** Siling Co. **c** Paiku Co. RMSE root-mean-square error, *r* correlation coefficient.

We further analyzed the factors affecting LSWT values in each month, as shown in Table 1. Air temperature exhibited a strong correlation with LSWTs in most months, especially in Nam Co and Siling Co, suggesting that air temperature substantially influences lake temperature on a monthly scale. However, the relationship between each meteorological variable and LSWTs varied considerably from month to month in Paiku Co. River

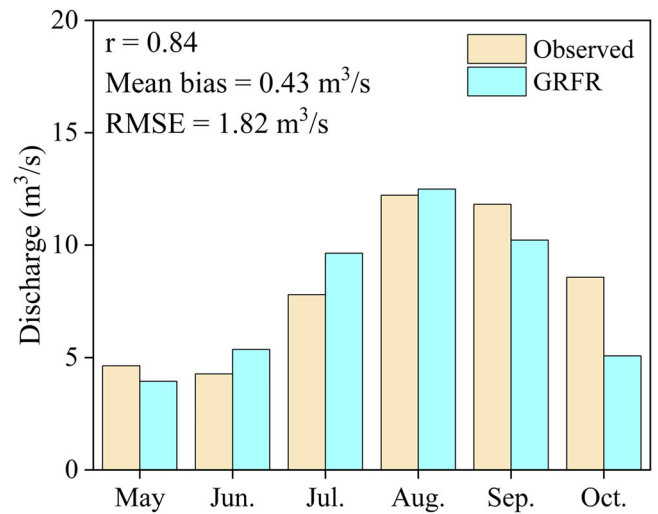


Fig. 4 | Comparison of multi-year monthly average values of discharge between observed and Global Reach-level Flood Reanalysis (GRFR) during the period 2008–2012 in Nam Co basin. RMSE root-mean-square error, *r* correlation.

discharge had a negative correlation with LSWTs in summer in all three lakes, indicative of the cooling effect of river inflows on LSWTs.

Intra-lake heterogeneity of LSWT and associated influencing factors

We calculated the summer and autumn LSWT averages in each lake for 19 years at the grid scale, and provided the locations of the major rivers flowing into the lake as well as the lake bathymetry corresponding to the lake. In general, the spatial distributions of LSWT exhibited notable differences across different seasons.

As illustrated in Fig. 7, the LSWT of Nam Co exhibits an obvious west-to-east warming gradient during summer. The eastern basin experiences higher temperatures due to its shallower depth and consequently lower heat capacity, allowing for faster thermal response. In contrast, the western margins exhibit cooler LSWT, likely resulting from wind-induced upwelling of colder subsurface waters driven by prevailing westerlies³⁶. In autumn, the temperature

of Nam Co shows a pattern where the central area is warmer while the surrounding areas are cooler. Near the lake inlet, the temperature is the lowest which may be associated with cooler inflow runoff. In autumn, the difference between the air temperature in the basin and the LSWT reached a maximum in October and November (Fig. 7d). There is a well-established positive correlation between river temperature and surrounding air temperature^{37,38}. Therefore, we used the difference between the basin average air temperature and LSWT as an indicator of the temperature difference between river and lake water. Our results indicate that the temperature difference between the lakes

and their inflowing rivers reached a peak during October and November, consistent with the findings of a previous study that measured lake and river temperatures in Paiku Co basin³⁵. In autumn, river water temperature experienced a rapid decline, whereas LSWT values remained relatively stable owing to the high specific heat capacity of lakes. Consequently, despite lower river inflow in autumn, the relatively cooler nature of the river water leads to sufficient cold water being brought into the lakes, resulting in the observed pattern of lower LSWT values at the inlets of the three lakes. The central lake region maintains higher temperatures due to its greater depth

Fig. 5 | Interannual variation of lake surface water temperature (LSWT). a Nam Co. b Siling Co. c Paiku Co.

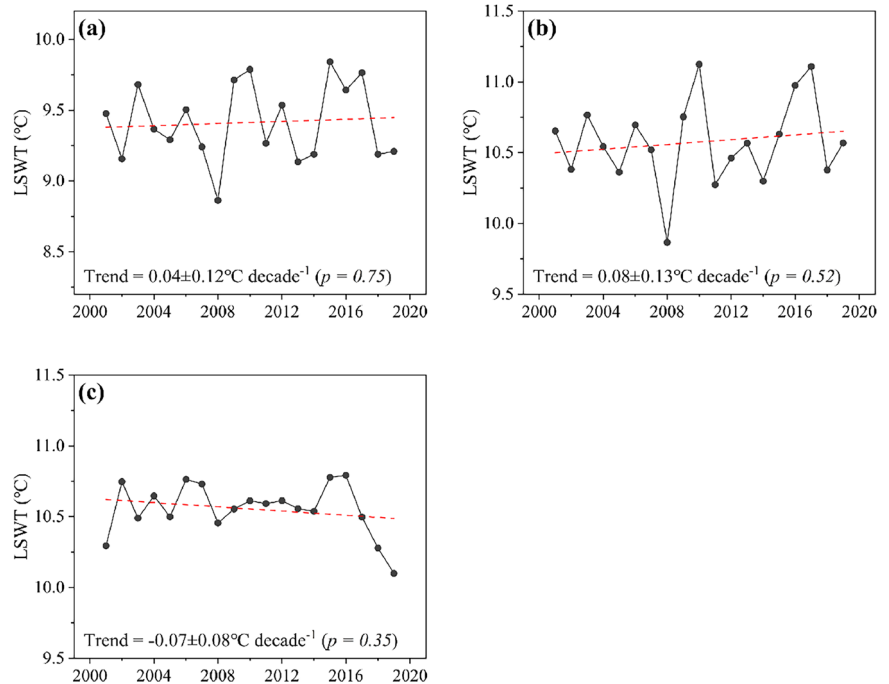
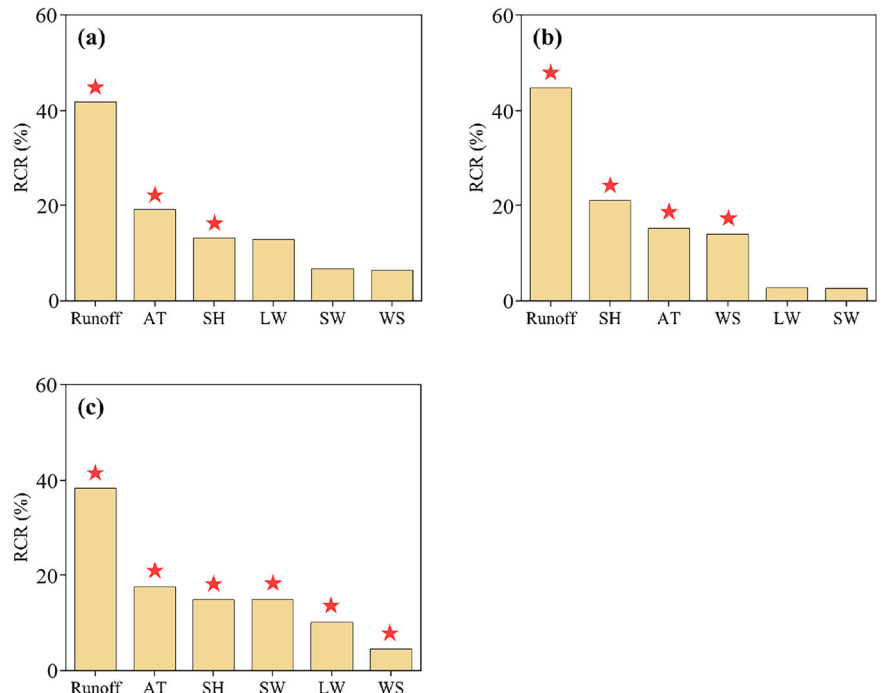


Fig. 6 | Estimated relative contribution rates (RCRs) of surface air temperature (AT), specific humidity (SH), 10 m wind speed (WS), shortwave radiation (SW), longwave radiation (LW), and runoff to long-term lake surface water temperatures (LSWTs) from July to November during the period 2001–2019. A red five-pointed star indicates that the corresponding variable passes the 95% significance test. a Nam Co. b Siling Co. c Paiku Co. The explained variances of random forest for the LSWT of Nam Co, Siling Co, and Paiku Co are 88.4%, 86.6%, and 88.3%, respectively.



(Fig. 7c), where the larger water volume provides increased heat capacity and slower cooling.

In Siling Co, rivers flow into it from all four compass directions. Among these, the Za'gya Zangbo in the northern basin and the Za'gen Zangbo and Ngari Zangbo in the western basin, which originate from mountain regions, have flow volumes that are over 20 times greater than those of rivers in the eastern and southern regions. Consequently, their cooling effects on LSWT in summer are more pronounced, resulting in two particularly cold zones: one with LSWT below 13 °C in

the northern part of the lake and another in the western part of the lake with an LSWT range of 13–13.3 °C (Fig. 8). In autumn, there is a significant temperature difference between the river and lake, causing lower temperatures near the inflow area of the lake.

In Paiku Co, the spatial distribution characteristics in summer and autumn are opposite (Fig. 9). In summer, the lowest lake temperatures occur in the northern region, attributable to its greater water depth which results in slower thermal response. The substantial river-lake temperature contrast in autumn induces lower temperatures in the southern lake region.

Table 1 | Correlation analysis between monthly mean air temperature (AT), downward longwave radiation (LW), downward shortwave radiation (SW), specific humidity (SH), wind speed (WS), discharge, and lake surface water temperature (LSWT) during the period 2001–2019

Lake	Time	AT	LW	SW	SH	WS	Discharge
Nam Co	Jul.	0.64	-0.35	0.56	-0.03	0.50	-0.67
	Aug.	0.25	0.02	0.15	0.26	0.13	-0.30
	Sep.	0.72	0.03	0.22	0.22	0.11	-0.02
	Oct.	0.73	0.03	0.32	0.26	0.36	-0.43
	Nov.	0.74	-0.38	0.27	-0.07	0.42	0.56
Siling Co	Jul.	0.37	0.31	-0.18	0.41	0.09	-0.15
	Aug.	0.52	-0.07	0.32	0.19	0.34	-0.20
	Sep.	0.63	-0.07	0.36	0.2	0.33	-0.17
	Oct.	0.71	-0.06	0.51	0.3	0.20	0.09
	Nov.	0.51	-0.16	0.14	-0.13	0.36	0.40
Paiku Co	Jul.	0.22	-0.23	0.24	-0.13	-0.06	-0.32
	Aug.	0.05	-0.07	0.10	0.02	-0.28	-0.11
	Sep.	0.44	0.35	-0.21	0.44	0.12	0.30
	Oct.	0.58	0.54	-0.21	0.63	0.09	0.50
	Nov.	0.22	0.14	0.06	0.26	-0.1	0.19

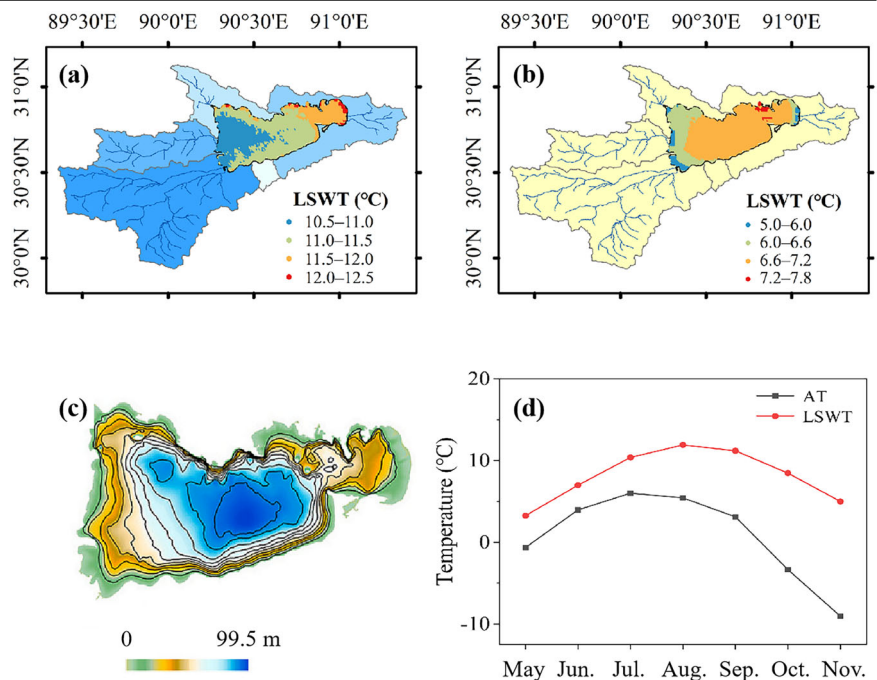
Bold numbers indicates that the 95% significance test has been passed.

Discussion

TP Lakes are sensitive to regional hydroclimatic changes and human activities. Studying the intra-lake heterogeneity of LSWT can help us to better understand regional environmental change. Our findings show that interannual variation of LSWT in Nam Co, Siling Co and Paiku Co was insignificant. The result of random forest analysis indicate that the factor with the greatest influence on LSWT in all three lakes was lake inflows, followed by air temperature and specific humidity from July to November. We found that lake inflows increased the intra-lake heterogeneity of LSWT, but the mechanism was different in summer compared with that in autumn. During summer, runoff flowing into the lakes significantly increased (Fig. 4), while in autumn, there is a large temperature difference between rivers and lakes. Both of these causing localized lower temperatures in certain areas of the lakes. In addition to runoff, the lake bathymetry can also explain the intra-lake heterogeneity of LSWT, which is manifested as the difference in LSWT between the deep and shallow areas of the lake.

The CCI-LSWT dataset is subject to inherent uncertainties from diverse sources. Radiative transfer models may introduce inaccuracies due to imperfect parameterizations or assumptions. Uncertainties associated with retrieval arise from simplifications in model design, observational constraints, or non-ideal atmospheric conditions. ERA5-Land dataset uncertainties stem from the model limitations in fully capturing the physical processes that govern the earth system. To evaluate how these uncertainties might affect the random forest results, we performed a sensitivity analysis by introducing Gaussian noise to each independent variable. The noise had a mean of 0 and a standard deviation equivalent to 10% of the standard

Fig. 7 | Intra-lake heterogeneity of lake surface water temperature (LSWT) and its influencing factors of Nam Co in summer and autumn.
a Spatial distribution of LSWT and location of rivers in summer at Nam Co Basin. Darker blue colors of catchments equate to larger river flows in the corresponding region. **b** The distribution of LSWT in autumn. **c** The bathymetry of Nam Co. **d** Variation of basin air temperature (AT) and LSWT.



deviation of the original variable. A total of 50 independent disturbance experiments were conducted. The results of the random forest model showed that the ranking of variable importance remained stable across all experiments. This indicates that the conclusions drawn from the model are robust and not significantly affected by the uncertainties in the input data.

This study emphasizes the influence of fluvial inflows on LSWT. In addition to precipitation, river inflow may originate from glacier and snow meltwater, particularly in the Tibetan Plateau region. Taking Nam Co as a case study (Fig. 10), we analyzed the intra-annual variations of total inflow runoff and cryospheric meltwater contribution (the sum of glacier and snow melt) from 2001 to 2019 based on the simulated results from Zhou et al.¹⁶

Result shows that the continuous influx of meltwater with a certain proportion from May to September constitutes a persistent cold water source entering the lake system, which may potentially contribute to LSWT suppression. Future climate warming may drive the contrasting thermal regimes in lake systems: In glacier-fed basins where glacier melt accelerates, an increase in cold meltwater fluxes may maintain or intensify the cooling effects of LSWT. Conversely, in regions where glacier retreat with declining meltwater contributions, the reduction of cold water injection may amplify lake warming trends. This bidirectional response highlights the critical role of cryospheric meltwater in modulating thermal dynamics of alpine lakes.

Fig. 8 | Intra-lake heterogeneity of lake surface water temperature (LSWT) and its influencing factors of Siling Co in summer and autumn.

a Spatial distribution of LSWT and location of rivers in summer at Siling Co Basin. Darker blue colors of catchments equate to larger river flows in the corresponding region. **b** The distribution of LSWT in autumn. **c** The bathymetry of Siling Co. **d** Variation of basin air temperature (AT) and LSWT.

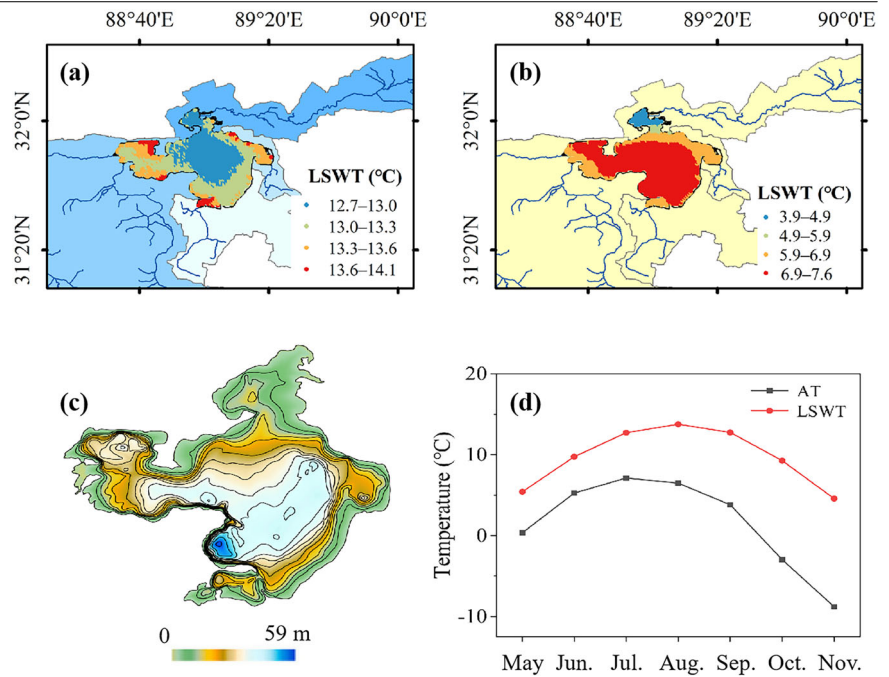
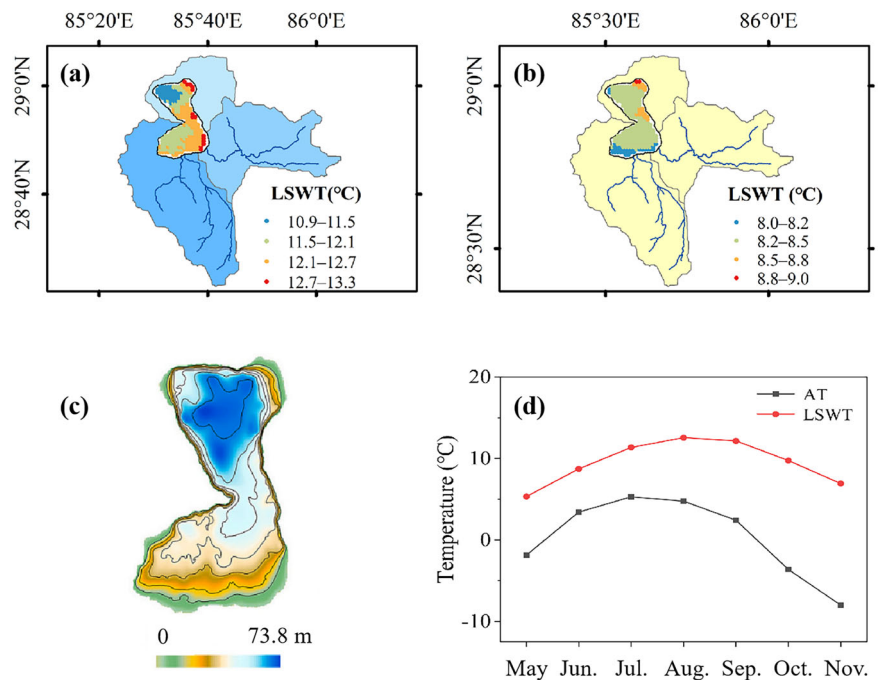


Fig. 9 | Intra-lake heterogeneity of lake surface water temperature (LSWT) and its influencing factors of Paiku Co in summer and autumn.

a Spatial distribution of LSWT and location of rivers in summer at Paiku Co Basin. Darker blue colors of catchments equate to larger river flows in the corresponding region. **b** The distribution of LSWT in autumn. **c** The bathymetry of Paiku Co. **d** Variation of basin air temperature (AT) and LSWT.



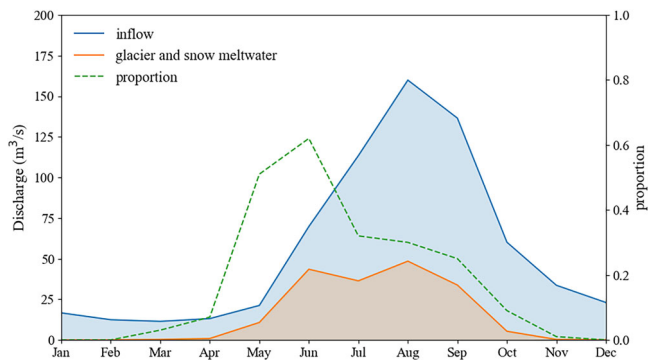


Fig. 10 | The intra-annual variability of total inflow runoff, glacier and snow meltwater, and the proportion of glacier and snow meltwater in the total inflow runoff in the Nam Co basin from 2001 to 2019.

The study of intra-lake heterogeneity of LSWT should be emphasized in future research because the spatial distribution of LSWT provides more insights than that a single average value of the whole lake. Meanwhile, future work needs more specific quantification of the relative contribution of river inflows, key meteorological factors (e.g., air temperature, wind speed) and lake bathymetry in shaping the heterogeneity of LSWT. A direct comparison using percentage contributions or significance testing would help to clarify the dominant drivers of spatial variation and further support the role of river inflows in lake thermodynamics. To achieve these objectives, the three-dimensional lake model should be encouraged, which is driven by external meteorological conditions such as wind stress, lake thermal stratification and basin topography, playing a critical role in shaping intra-lake LSWT heterogeneity^{39–41}.

Methods

Study area

The main study area comprised three lakes located on the central and southern parts of the TP: Nam Co, Siling Co, and Paiku Co. Nam Co, with a surface area of over 2000 km², is situated to the north of the Nyainqentanglha Mountains. The main rivers flowing into Nam Co are the Naqu, Boqu, Angqu, and Cequ on the western shoreline, the Niyaqu on the eastern shoreline, and a series of parallel tributaries on the southern shoreline, few rivers flow into the northern part of the lake. The lake gradually becomes shallower from the center to the periphery, with a maximum depth exceeding 90 m and an average depth of over 50 m³³. The average annual temperature of Nam Co is below 0 °C, with the highest temperature occurring in July⁴². Glacial meltwater is of great importance to the water balance and hydrological processes within Nam Co and its surrounding basin^{43,44}. Siling Co is currently the largest lake in the Tibet Autonomous Region of China⁴⁵. This lake is located within a closed catchment, with the main rivers flowing into it being the Za'gen Zangbo and Ngari Zangbo in the west, Boques Zangbo in the east, and Za'gya Zangbo in the north. The average annual temperature of Siling Co is 0.3 °C and the average total annual rainfall is approximately 290 mm. Lake inflow is markedly affected by both precipitation and snow and glacier melt⁴⁶. Paiku Co, located on the southern TP, is also a hydrologically closed lake and has a surface area of 266 km². Rivers flow from south to north into the lake; major rivers include the Daqu, Bulaqu, and Barixiongqu. The average depth of the lake is 41.1 m and the deepest point (72.8 m) is located in the northern portion of the lake⁴⁷. According to the second Chinese glacier inventory in 2009⁴⁸, the total glacial area in Paiku Co basin has decreased from 130.2 to 119.9 km² during the past 40 years. The average annual air temperature from June 2015 to May 2016 was 4.4 °C⁴⁷.

Observational data

In-situ measured lake water temperature data for the three lakes were obtained from the National Tibetan Plateau/Third Pole Environment Data

Center. In-situ water temperature monitoring data (3–83 m in depth, 10 layers) for Nam Co (Fig. 1b) were collected from October 2011 to July 2014⁴⁹, and expressed as daily average values. Daily lake water temperature measurements (2–38 m in depth, 5 layers) for Siling Co (Fig. 1c) spanned the period June–December 2017. Using the observed lake water temperature data from different depths in Nam Co and Siling Co, model curves were constructed to obtain the lake water temperature at 0 m when data from all depths were available. In total, 48 data points were available for Nam Co, while 93 data points were available for Siling Co. In Paiku Co (Fig. 1d), two water temperature profiles were monitored: one in the southern part of the lake (0–42 m in depth) and the other in the northern part (0–72 m in depth)³⁵. These observed data spanned the period June 2015–May 2018 for the southern monitoring point, and June 2016–May 2017 for the northern monitoring point. The observed water temperature data at 0 m for the three lakes were used to validate LSWT product data.

In addition to lake water temperature data, observed daily runoff data in the Niyaqu River, located in the eastern part of the Nam Co basin (Fig. 1b), were collected. The observed runoff data were obtained from the Nam Co Monitoring and Research Station for Multisphere Interactions (30°46'N, 90°59'E), which was established by the Institute of Tibetan Plateau Research, Chinese Academy of Sciences in 2005. These data, available from May to October over the period 2008–2012, were primarily used to validate lake inflow data from runoff products.

Following the method described in Han et al.⁵⁰, the bathymetry of three lakes was derived from vectorized contour lines based on prior surveys^{47,51,52}, and was mainly used to evaluate its impact on the intra-lake heterogeneity of LSWT.

Product-based LSWT data

A satellite-derived LSWT product with high spatial resolution, released by the European Space Agency Climate Change Initiative (CCI-LSWT)^{53–55}, has been widely used in previous studies^{6,56,57} and was also utilized here. The CCI-LSWT dataset provides daily LSWT data for 2024 lakes worldwide from five sensors: ATSR2 (ERS-2), AATSR (Envisat), MODIS (Terra), AVHRR (MetOpA and MetOpB) and SLSTR (Sentinel3A and Sentinel3B), with a spatial resolution of 1/120° grid format (~1 km resolution at the equator). For the three studied lakes, a buffer zone of 1 km was constructed to eliminate the influence of water level change on LSWT.

The CCI-LSWT data are sparse during the ice-covered period owing to problems in discriminating clouds from lake ice or snow⁵⁸. Hence, we only analysis the lake water temperature in summer (July–September) and autumn (October–November)^{12,59}, excluding December because the lakes are generally frozen at this time^{33–35}. The CCI-LSWT dataset was validated at the point scale. By identifying the four nearest grid points corresponding to the in-situ measurement locations of each lake, we compared the measured lake temperatures at 0 m with the mean CCI-LSWT values of these four grid points.

Validation of water surface temperatures from the MODIS land surface temperature (LST) product against in-situ measurements has been conducted in previous studies, showing good performance for many lakes^{60–62}. Therefore, the MODIS LST product was used here to validate the CCI-LSWT product in terms of the overall LSWT variations in the three lakes. The MODIS LST dataset contains 15 years (2001–2015) of nighttime and daytime LSWT data for 374 lakes²². For comparison with the CCI-LSWT dataset, we specifically utilized the daytime LSWT data obtained from each entire lake.

Meteorological data

The European Centre for Medium-range Weather Forecasts (ECMWF) Reanalysis v5-Land (ERA5-Land) dataset⁶³ provides global land gridded climate-forcing data from 1981 to the near present at hourly temporal resolution and a spatial resolution of 0.1° × 0.1°. Various climate-forcing variables from the hourly ERA5-Land dataset were used to analyze their influence on LSWT. On the basis of previous work^{7,30}, we selected five factors that mainly influence LSWT: 2-m air temperature, longwave radiation,

shortwave radiation, wind speed, and specific humidity. Wind speed was calculated using both the 10 m v-component and u-component of wind. Specific humidity was accurately estimated by integrating the 2 m dewpoint temperature and surface pressure data. For each lake, the monthly mean value of each meteorological variable was calculated.

Lake inflows

Lake inflow data were derived from the Global Reach-level Flood Reanalysis (GRFR) dataset, which contains 3-hourly and daily river flow records for 2.94 million rivers worldwide over a 40-year period from 1980 to 2019⁶⁴. The dataset is based on the variable infiltration capacity distributed hydrological model and the parallel computation of discharge model, integrating global natural river runoff with high resolution and accuracy into simulations. For each lake basin, we extracted lake inflow data from major rivers that flow into the lakes and calculated the monthly average river discharge from the GRFR dataset. For Niyaqu River in Nam Co Basin, the multi-year monthly average observed runoff (calculated from daily data) was compared with the lake inflow obtained from the GRFR product (Fig. 4).

Basin boundaries

Lake basin boundaries were obtained from the HydroBASINS dataset, which offers 12 hierarchically nested sub-basin breakdowns globally at arc-second resolution⁶⁵. Level six and seven watersheds were mainly used here.

Estimating the contributions of forcing variables to LSWT

In this study, our predictors used in random forest included meteorological variables (wind speed, air temperature, shortwave radiation, longwave radiation, and specific humidity) as well as river discharge. We used zero-phase component analysis to eliminate the effects of interactions among variables as much as possible. This method is commonly used for data preprocessing in machine learning and has also been applied to the reconstruction of climate fields⁶⁶. The random forest method was then used to estimate the contributions of hydrometeorological variables to changes in LSWT values. Random forest is a classification tree-based algorithm that falls under the broader category of machine learning methods, requiring simulation and iterative processes. Breiman⁶⁷ introduced the Bagging (Bootstrap Aggregation) method, which became a milestone in the field of machine learning and has been widely cited. Based on the Bagging approach that randomly selects subsets of samples, the random forest algorithm further reduces the correlation between individual trees by randomly selecting features at each node. This enhances regression accuracy and improves overall model performance. Compared with other statistical classifiers, random forest offers advantages such as high classification accuracy, ability to model complex interactions among predictor variables, and flexibility in performing various types of statistical data analyses⁶⁸. The order of importance was determined by their frequency and relative position in individual trees across the entire forest. The explanatory power of the response variables was estimated using the mean-squared error (MSE). Subsequently, the relative contribution rate (RCR) of each factor was calculated based on the MSE values. Random forest has been applied to lake feature attribution in previous studies^{69,70}.

Evaluation criteria

Various statistical criteria, including root-mean-square error (RMSE), bias, and correlation coefficient (r) were used to evaluate the performances of the CCI-LSWT and GRFR runoff products. These criteria are defined as follows:

$$RMSE = \sqrt{\sum_{i=1}^N (X_{s,t} - X_{o,t})^2 / N}, \quad (1)$$

$$Bias = \sum_{i=1}^N (X_{s,t} - X_{o,t}) / N, \quad (2)$$

$$r = \left[\sum_{i=1}^N (X_{s,t} - \bar{X}_s)(X_{o,t} - \bar{X}_o) \right] / \left[\sqrt{\sum_{i=1}^N (X_{s,t} - \bar{X}_s)^2} \sqrt{\sum_{i=1}^N (X_{o,t} - \bar{X}_o)^2} \right], \quad (3)$$

where, N is the number of observed values; $X_{s,t}$ includes both observed and MODIS LSWT values, as well as observed runoff values at Niyaqu at t moment; $X_{o,t}$ represents CCI-LSWT and runoff values from GRFR; \bar{X}_s and \bar{X}_o denotes the mean value of the corresponding data.

Data availability

The data used in this paper and their available sources are as follows. In-situ measured lake water temperature data in Nam Co, Siling Co and Paiku Co were obtained from <https://doi.org/10.11888/Hydro.tpd.270332>, <https://doi.org/10.11888/Hydro.tpd.270083>, <https://doi.org/10.11888/Hydro.tpd.270287> respectively. CCI-LSWT can be accessed at https://climate.esa.int/en/projects/lakes/news-and-events/news/first-lakes_cci-dataset-now-available/. The Global Reach-Level 3-Hourly River Flood Reanalysis (GRFR) data were obtained from <https://www.reachhydro.org/home/records/grfr>. The ERA5-Land data are freely available from <https://cds.climate.copernicus.eu/datasets/reanalysis-era5-land-monthly-means?tab=overview>. Lake basin boundaries were obtained from the <https://www.hydrosheds.org/products/hydrobasins>.

Code availability

The source codes for the analysis of this study are available from the corresponding author upon reasonable request.

Received: 1 November 2024; Accepted: 7 May 2025;

Published online: 24 May 2025

References

- Gleick, P. H. Water and conflict: Fresh water resources and international security. *Int. Security (U.S.A.)* **18**, 79–112 (1993).
- Tranvik, L. J. et al. Lakes and reservoirs as regulators of carbon cycling and climate. *Limnol. Oceanogr.* **54**, 2298–2314 (2009).
- Adrian, R. et al. Lakes as sentinels of climate change. *Limnol. Oceanogr.* **54**, 2283–2297 (2009).
- Sharma, S. et al. Widespread loss of lake ice around the Northern Hemisphere in a warming world. *Nat. Clim. Change* **9**, 227–231 (2019).
- Huang, L. et al. Emerging unprecedented lake ice loss in climate change projections. *Nat. Commun.* **13**, 5798 (2022).
- Li, X., Peng, S., Xi, Y., Woolway, R. I. & Liu, G. Earlier ice loss accelerates lake warming in the Northern Hemisphere. *Nat. Commun.* **13**, 5156 (2022).
- Tong, Y. et al. Global lakes are warming slower than surface air temperature due to accelerated evaporation. *Nat. Water* **1**, 929–940 (2023).
- Woolway, R. I. & Merchant, C. J. Worldwide alteration of lake mixing regimes in response to climate change. *Nat. Geosci.* **12**, 271–276 (2019).
- Carrea, L. et al. Lake surface water temperature. *Bull. Am. Meteorol. Soc.* **105**, S33–S34 (2024).
- O'Reilly, C. M. et al. Rapid and highly variable warming of lake surface waters around the globe. *Geophys. Res. Lett.* **42**, 10,773–710,781 (2015).
- Huang, L. et al. Emergence of lake conditions that exceed natural temperature variability. *Nat. Geosci.* **17**, 763–769 (2024).
- Sharma, S. et al. A global database of lake surface temperatures collected by in situ and satellite methods from 1985–2009. *Sci. Data* **2**, 150008 (2015).
- Yan, F. et al. Lakes on the Tibetan Plateau as Conduits of Greenhouse Gases to the Atmosphere. *J. Geophys. Res.: Biogeosci.* **123**, 2091–2103 (2018).
- Yao, T. et al. Recent Third Poleas Rapid Warming Accompanies Cryospheric Melt and Water Cycle Intensification and Interactions

- between Monsoon and Environment: Multidisciplinary Approach with Observations, Modeling, and Analysis. *Bull. Am. Meteorol. Soc.* **100**, 423–444 (2019).
15. Lei, Y. et al. Response of inland lake dynamics over the Tibetan Plateau to climate change. *Clim. Chang.* **125**, 281–290 (2014).
 16. Zhou, J. et al. Quantifying the major drivers for the expanding lakes in the interior Tibetan Plateau. *Sci. Bull.* **67**, 474–478 (2022).
 17. Zhang, G., Xie, H., Kang, S., Yi, D. & Ackley, S. F. Monitoring lake level changes on the Tibetan Plateau using ICESat altimetry data (2003–2009). *Remote Sens. Environ.* **115**, 1733–1742 (2011).
 18. Song, C., Ye, Q., Sheng, Y. & Gong, T. Combined ICESat and CryoSat-2 Altimetry for Accessing Water Level Dynamics of Tibetan Lakes over 2003–2014. *Water* **7**, 4685–4700 (2015).
 19. Wu, Y., Zhang, X., Zheng, H., Li, J. & Wang, Z. Investigating changes in lake systems in the south-central Tibetan Plateau with multi-source remote sensing. *J. Geographical Sci.* **27**, 337–347 (2017).
 20. Yang, K. et al. Quantifying recent precipitation change and predicting lake expansion in the Inner Tibetan Plateau. *Climatic Change* **147**, 149–163 (2018).
 21. Zhang, G. et al. Estimating surface temperature changes of lakes in the Tibetan Plateau using MODIS LST data. *J. Geophys. Res.: Atmospheres* **119**, 8552–8567 (2014).
 22. Wan, W. et al. A comprehensive data set of lake surface water temperature over the Tibetan Plateau derived from MODIS LST products 2001–2015. *Sci. Data* **4**, 170095 (2017).
 23. Guo, L. et al. An integrated dataset of daily lake surface water temperature over the Tibetan Plateau. *Earth Syst. Sci. Data* **14**, 3411–3422 (2022).
 24. Jia, T. et al. Review on the Change Trend, Attribution Analysis, Retrieval, Simulation, and Prediction of Lake Surface Water Temperature. *IEEE J. Sel. Top. Appl. Earth Observations Remote Sens.* **15**, 6324–6355 (2022).
 25. Pilla, R. M. et al. Deeper waters are changing less consistently than surface waters in a global analysis of 102 lakes. *Sci. Rep.* **10**, 20514 (2020).
 26. Jane, S. F. et al. Widespread deoxygenation of temperate lakes. *Nature* **594**, 66–70 (2021).
 27. Woolway, R. I. et al. Lake heatwaves under climate change. *Nature* **589**, 402–407 (2021).
 28. Schmid, M. & Köster, O. Excess warming of a Central European lake driven by solar brightening. *Water Resour. Res.* **52**, 8103–8116 (2016).
 29. Huang, A., Rao, Y. R. & Zhang, W. On Recent Trends in Atmospheric and Limnological Variables in Lake Ontario. *J. Clim.* **25**, 5807–5816 (2012).
 30. Huang, L. et al. Attribution of Lake Surface Water Temperature Change in Large Lakes Across China Over Past Four Decades. *J. Geophys. Res.: Atmospheres* **128**, e2022JD038465 (2023).
 31. Zhang, G. Q. et al. Response of Tibetan Plateau lakes to climate change: Trends, patterns, and mechanisms. *Earth-Sci. Rev.* **208**, 103269 (2020).
 32. Woolway, R. I. & Merchant, C. J. Intralake Heterogeneity of Thermal Responses to Climate Change: A Study of Large Northern Hemisphere Lakes. *J. Geophys. Res.: Atmospheres* **123**, 3087–3098 (2018).
 33. Shi, Y. et al. Drivers of Warming in Lake Nam Co on Tibetan Plateau Over the Past 40 Years. *J. Geophys. Res.: Atmospheres* **127**, e2021JD036320 (2022).
 34. Ke, L. & Song, C. Remotely sensed surface temperature variation of an inland saline lake over the central Qinghai–Tibet Plateau. *ISPRS J. Photogramm. Remote Sens.* **98**, 157–167 (2014).
 35. Lei, Y. et al. Contrasting hydrological and thermal intensities determine seasonal lake-level variations – a case study at Paiku Co on the southern Tibetan Plateau. *Hydrol. Earth Syst. Sci.* **25**, 3163–3177 (2021).
 36. Wu, Y. et al. Numerical Study of the Thermal Structure and Circulation in a Large and Deep Dimictic Lake Over Tibetan Plateau. *J. Geophys. Res.: Oceans* **126**, e2021JC017517 (2021).
 37. Segura, C., Caldwell, P., Sun, G., McNulty, S. & Zhang, Y. A model to predict stream water temperature across the conterminous USA. *Hydrological Process.* **29**, 2178–2195 (2015).
 38. Bachmann, R. W., Canfield, D. E., Sharma, S. & Lecours, V. Warming of Near-Surface Summer Water Temperatures in Lakes of the Conterminous United States. *Water* **12**, 3381 (2020).
 39. Xue, P., Schwab, D. J. & Hu, S. An investigation of the thermal response to meteorological forcing in a hydrodynamic model of Lake Superior. *J. Geophys. Res.: Oceans* **120**, 5233–5253 (2015).
 40. Xue, P. et al. Improving the Simulation of Large Lakes in Regional Climate Modeling: Two-Way Lake–Atmosphere Coupling with a 3D Hydrodynamic Model of the Great Lakes. *J. Clim.* **30**, 1605–1627 (2017).
 41. Wu, Y. et al. Application of a Three-Dimensional Coupled Hydrodynamic–Ice Model to Assess Spatiotemporal Variations in Ice Cover and Underlying Mechanisms in Lake Nam Co, Tibetan Plateau, 2007–2017. *J. Geophys. Res.: Atmospheres* **128**, e2023JD038844 (2023).
 42. Gao, T.-g et al. Stream temperature dynamics in Nam Co basin, southern Tibetan Plateau. *J. Mt. Sci.* **14**, 2458–2470 (2017).
 43. Tanguang, G. et al. Simulation and analysis of glacier runoff and mass balance in the Nam Co basin, southern Tibetan Plateau. *J. Glaciol.* **61**, 447–460 (2015).
 44. Adnan, M. et al. Simulation and Analysis of the Water Balance of the Nam Co Lake Using SWAT Model. *Water* **11**, 1383 (2019).
 45. Zhu, L. et al. Climatic and lake environmental changes in the Serling Co region of Tibet over a variety of timescales. *Sci. Bull.* **64**, 422–424 (2019).
 46. Zhou, J. et al. Exploring the water storage changes in the largest lake (Selin Co) over the Tibetan Plateau during 2003–2012 from a basin-wide hydrological modeling. *Water Resour. Res.* **51**, 8060–8086 (2015).
 47. Lei, Y. et al. An integrated investigation of lake storage and water level changes in the Paiku Co basin, central Himalayas. *J. Hydrol.* **562**, 599–608 (2018).
 48. Junfeng, W. et al. Surface-area changes of glaciers in the Tibetan Plateau interior area since the 1970s using recent Landsat images and historical maps. *Ann. Glaciol.* **55**, 213–222 (2014).
 49. Wang, J. et al. Spatial and temporal variations in water temperature in a high-altitude deep dimictic mountain lake (Nam Co), central Tibetan Plateau. *J. Gt. Lakes Res.* **45**, 212–223 (2019).
 50. Han, X. et al. Reconstructing Tibetan Plateau lake bathymetry using ICESat-2 photon-counting laser altimetry. *Remote Sens. Environ.* **315**, 114458 (2024).
 51. Gyawali, A. R. et al. Paleo-environmental change since the Late Glacial inferred from lacustrine sediment in Selin Co, central Tibet. *Palaeogeogr., Palaeoclimatol., Palaeoecol.* **516**, 101–112 (2019).
 52. Wang, J. et al. Seasonal stratification of a deep, high-altitude, dimictic lake: Nam Co, Tibetan Plateau. *J. Hydrol.* **584**, 124668 (2020).
 53. Crétaux, J. et al. ESA Lakes climate change initiative (Lakes_cci): lake products, version 1.0. Centre for Environmental Data Analysis (2020).
 54. Carrea, L. et al. ESA Lakes Climate Change Initiative (Lakes_cci): Lake Products, Version 2.0. NERC EDS Centre for Environmental Data Analysis. (2022).
 55. Carrea, L. et al. Satellite-derived multivariate world-wide lake physical variable timeseries for climate studies. *Sci. Data* **10**, 30 (2023).
 56. Woolway, R. I. et al. Phenological shifts in lake stratification under climate change. *Nat. Commun.* **12**, 2318 (2021).
 57. Woolway, R. I., Albergel, C., Frölicher, T. L. & Perroud, M. Severe Lake Heatwaves Attributable to Human-Induced Global Warming. *Geophys. Res. Lett.* **49**, e2021GL097031 (2022).
 58. Lazhu et al. Quantifying evaporation and its decadal change for Lake Nam Co, central Tibetan Plateau. *J. Geophys. Res. Atmospheres* **121**, 7578–7591 (2016).
 59. Schneider, P. & Hook, S. J. Space observations of inland water bodies show rapid surface warming since 1985. *Geophys. Res. Lett.* **37**, L22405 (2010).

60. Reinart, A. & Reinhold, M. Mapping surface temperature in large lakes with MODIS data. *Remote Sens. Environ.* **112**, 603–611 (2008).
61. Schneider, P. et al. Satellite observations indicate rapid warming trend for lakes in California and Nevada. *Geophys. Res. Lett.* **36**, 22 (2009).
62. Hulley, G. C., Hook, S. J. & Schneider, P. Optimized split-window coefficients for deriving surface temperatures from inland water bodies. *Remote Sens. Environ.* **115**, 3758–3769 (2011).
63. Muñoz Sabater, J. ERA5-Land hourly data from 1981 to present, Copernicus Climate Change Service (C3S) Climate Data Store (CDS) [data set] (2019).
64. Yang, Y. et al. Global Reach-Level 3-Hourly River Flood Reanalysis (1980-2019). *Bull. Am. Meteorol. Soc.* **102**, E2086–E2105 (2021).
65. Lehner, B. & Grill, G. Global river hydrography and network routing: baseline data and new approaches to study the world's large river systems. *Hydrol. Process.* **27**, 2171–2186 (2013).
66. Bocinsky, R. K. & Kohler, T. A. A 2,000-year reconstruction of the rain-fed maize agricultural niche in the US Southwest. *Nat. Commun.* **5**, 5618 (2014).
67. Breiman, L. Random Forests. *Mach. Learn.* **45**, 5–32 (2001).
68. Cutler, D. R. et al. Random forests for classification in ecology. *Ecology* **88**, 2783–2792 (2007).
69. Zhou, J. et al. Controls of thermal response of temperate lakes to atmospheric warming. *Nat. Commun.* **14**, 6503 (2023).
70. Liu, D. et al. Substantial increase of organic carbon storage in Chinese lakes. *Nat. Commun.* **15**, 8049 (2024).

Acknowledgements

We thank Dr. Guoshuai Zhang (Institute of Tibetan Plateau Research, Chinese Academy of Sciences), who provided the in-situ observed lake inflow data (for Nam Co basin). We acknowledge the valuable comments and suggestions made by the editor and anonymous reviewers, which helped to improve this manuscript. This research was supported by the Second Tibetan Plateau Scientific Expedition and Research Program (grant 2024QZKK0400) and National Natural Science Foundation of China (grants U2202208 and 42471044).

Author contributions

W.L. and Z.J. conceived and designed the study. D.B. performed the analyses, and wrote the first draft of the manuscript. All co-authors reviewed and edited the manuscript.

Competing interests

The authors declare no competing interests.

Additional information

Correspondence and requests for materials should be addressed to Jing Zhou or Lei Wang.

Reprints and permissions information is available at <http://www.nature.com/reprints>

Publisher's note Springer Nature remains neutral with regard to jurisdictional claims in published maps and institutional affiliations.

Open Access This article is licensed under a Creative Commons Attribution-NonCommercial-NoDerivatives 4.0 International License, which permits any non-commercial use, sharing, distribution and reproduction in any medium or format, as long as you give appropriate credit to the original author(s) and the source, provide a link to the Creative Commons licence, and indicate if you modified the licensed material. You do not have permission under this licence to share adapted material derived from this article or parts of it. The images or other third party material in this article are included in the article's Creative Commons licence, unless indicated otherwise in a credit line to the material. If material is not included in the article's Creative Commons licence and your intended use is not permitted by statutory regulation or exceeds the permitted use, you will need to obtain permission directly from the copyright holder. To view a copy of this licence, visit <http://creativecommons.org/licenses/by-nc-nd/4.0/>.

© The Author(s) 2025